Afyon Kocatepe Üniversitesi Fen ve Mühendislik Bilimleri Dergisi
Afyon Kocatepe University – Journal of Science and Engineering
https://dergipark.org.tr/tr/pub/akufemubid

Araştırma Makalesi / Research Article
DOI: https://doi.org/10.35414/akufemubid.1446467
AKÜ FEMÜBİD **24** (2024) 065201 (1395-1402)
AKU J. Sci. Eng. **24** (2024) 065201 (1395-1402)

Tunable Ultra-wideband Band-stop Filters Based on a Metal-insulator-metal Waveguide with Triangle Resonators

Makale Bilgisi / Article Info
Alındı/Received: 04.03.2024
Kabul/Accepted: 05.08.2024
Yayımlandı/Published: xx.xx.xxxx

Üçgen Rezonatörlü Metal-yalıtkan-metal Dalga Kılavuzu Temelli Ayarlanabilir Ultra-genişbant Bant Durdurma Filtreleri

Semih KORKMAZ*

Bandırma Onyedi Eylul University, Faculty of Engineering and Natural Sciences, Department of Computer Engineering, Balıkesir, Türkiye

Abstract

This study introduces the design and analysis of ultra-wideband band-stop filters based on a metal-insulator-metal (MIM) waveguide with triangle resonators. The optical features of the filters have been determined numerically. Transmission values and field distributions of the filters have been obtained. To show the tunability of the resonances of the filters, parameter sweep analysis has been done. This feature provides the shifted wideband bandwidths from visible to mid-infrared regimes. Analyses have been carried out for three different designs. While the designs are analyzed, higher bandwidths are obtained by increasing the number and dimensions of the triangle resonators in the structure. The highest bandwidth is 859 nm for band-stop filtering in this work. This research can potentially improve the filtering capabilities of optical devices that use high-efficiency MIM waveguide-resonator systems.

Keywords: *Ultra-wideband; Bandwidth; Triangle resonators; Transmission; Field distributions; Band-stop filter*.

Öz

Bu çalışma, üçgen rezonatörlü metal-yalıtkan-metal (MIM) dalga kılavuzu temelli ultra-genişbant bant durdurma filtrelerinin tasarımını ve analizini tanıtmaktadır. Filtrelerin optik özellikleri nümerik olarak belirlenmiştir. Filtrelerin iletim değerleri ve alan dağılımları elde edilmiştir. Filtrelerin rezonanslarının ayarlanabilirliğini göstermek için parametre tarama analizi yapılmıştır. Bu özellik, genişbant bant genişliklerinin görünürden orta kızılötesi bölgelere kaydırılmasını sağlar. Analizler, üç farklı tasarım için gerçekleştirilmiştir. Tasarımlar analiz edilirken, yapıdaki üçgen rezonatörlerinin sayılarının ve boyutlarının arttırılmasıyla daha yüksek bant-genişlikleri elde edilmiştir. Bu çalışmada, bant-durdurma filtrelemesi için en yüksek bant genişliği 859 nm'dir. Bu araştırma, yüksek verimli MIM dalga kılavuzu-rezonatör sistemlerini kullanan optik cihazların filtreleme yeteneklerini geliştirme potansiyeline sahiptir.

Anahtar Kelimeler:*Ultra-genişbant; Bant genişliği; Üçgen rezonatörler; İletim; Alan dağılımları; Bant-durdurma filtresi*

1. Introduction

The need for compact and efficient photonic devices that can process light with high precision has increased research on new structures in recent years [Tan *et al*. 2021, Lin *et al*. 2020, Luo *et al*. 2023]. Optical filters based on metal-insulator-metal (MIM) waveguides stand out as key components to control the light [Korkmaz 2024, Haque *et al*. 2024, Zeng *et al*. 2022]. In particular, the integration of MIM waveguides with resonators has received much interest thanks to its potential to achieve broadband spectral control and multi-purpose filtering capabilities [Chou *et al*. 2020, Patel *et al*. 2022, Chao *et al*. 2022, Ebadi *et al*. 2020]. This relationship offers an efficient platform for designing band-stop filters with tunable frequencies [Mohammadi *et al*. 2023, Liu *et al*. 2024]. Propagating waves within the MIM waveguide coupled with resonators makes it possible to realize band-stop functionalities over a wide range of frequencies. For that purpose, ultra-wideband band-stop filter designs have been proposed with various shapes of nanoresonators which are hexagonal resonators [Zegaar *et al*. 2024], multi-circular ring resonators [Kamari *et al*. 2021], T-shaped resonators [Kamari *et al*. 2021], double-side trapezoidal resonators [Yu *et al*. 2020].

Triangle resonators are utilized for different applications which are band-pass filters [Mariselvam *et al*. 2022], switches [Zhang *et al*. 2022], absorbers [Ebadi *et al*. 2023], and sensors [Al Mahmud *et al.* 2021]. In this study, ultra-wideband band-stop filters based on a MIM waveguide with triangle resonators have been designed. These filters are analyzed numerically by the finite difference time domain (FDTD) method and have tunable resonances. During calculations, Lumerical FDTD solutions software is utilized [Int. Ref. 1]. The basic structure that has a metal-insulator-metal waveguide with triangle resonators has been investigated with the parameter sweep in the first step. By using the obtained ideal geometric parameters, three different ultra-wideband band-stop filters have

* *Sorumlu Yazar/Corresponding Author: Semih Korkmaz* *e-posta/e-mail:semihkorkmaz@bandirma.edu.tr*

been designed and the bandwidths of the filters have been determined in the second step. Field distributions at the corresponding resonance wavelengths are visualized to show the band-stop feature of the filters. Increasing the number of adjacent resonators to the waveguide provides the larger bandwidths. This study presents important results in ultra-wideband filter designs. With high parameter sensitivity, it shows adjustable band-stop regions in the desired range from the visible region to the infrared region. The highest bandwidth is obtained as 859 nm. When the designed ultra-wideband band-stop filters are compared to the literature, the attained results are promising for effective tools in integrated optical circuits.

2. Design and Analysis Method

Figure 1(a) presents the basic filter design. The design has a 150 nm-thick metal plate with a 50 nm width straight waveguide and triangle resonators. The triangle resonators are positioned adjacent to the waveguide. For the lengths of the resonator, L_1 and L_2 are 225 nm and 200 nm, respectively. Perfectly matched layer (PML) boundary conditions are utilized for x and y-axes. The yellow and white areas on the proposed design are metal and air, respectively. The design is analyzed with the Johnson and Christy model for optical constants of the silver metal [Johnson and Christy 1972]. The refractive index of air is 1. Transverse magnetic polarized Gaussian light is transmitted along the straight waveguide. The transmission values of the proposed design are numerically attained. The transmission spectrum of the structure is obtained with the formula (1) [Chao *et al*. 2022].

$$T = \frac{P_{out}}{P_{in}} \quad (1)$$

Here, P_{in} and P_{out} indicate input and output power, respectively. The wavelength of the Gaussian light is larger than the width of the designed waveguide. So, the waveguide supports only a single transverse magnetic (TM_0) mode. The resonance wavelength of the resonator for the TM_0 mode can be determined in the formula (2) [Zegaar *et al*. 2022].

$$\lambda_m = \frac{2R_e(n_{eff})L_{eff}}{m}, m = 1,2,3, \dots \dots \quad (2)$$

In the formula, $R_e(n_{eff})$ indicates the real part of the effective refractive index of the surface plasmon polariton. L_{eff} describes the effective resonance length of the resonator and m is the mode number. Figure 1(b) presents resonance wavelengths at 467.5 nm and 828.3 nm with zero transmission. This figure also shows magnetic field distributions ($|H|/|H_{in}|$) for the resonant wavelengths. While the electromagnetic waves are stopped at 467.5 nm and 828.3 nm with zero transmission, they are transmitted at 615 nm and 1500 nm where the transmission values reach 95%.

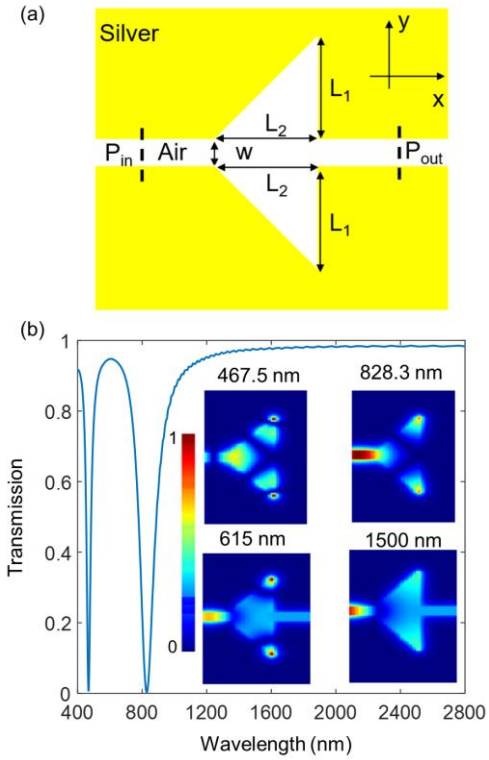

Figure 1. (a) The view of basic filter design. The x-axis length and the y-axis length are 1 µm for the structure. (b) The transmission spectrum and field distributions at different resonance wavelengths.

3. Results and Discussions

In the first step, the optimal geometrical parameter is obtained by parameter sweep. For this structure, the L_1 lengths of the resonators are critical to determine the resonance wavelengths. Only the L_1 lengths of the resonator are changed because the transmission spectra are mainly determined by the interaction of electromagnetic signals with L_1. Figure 2 shows the parameter sweep for L_1 lengths while other parameters are fixed and L_2 and w are 200 nm and 50 nm, respectively. The resonance wavelengths shift to longer wavelengths without any change in transmission values when L_1 length is increased from 210 nm to 240 nm with a 10 nm increment. This parameter sweep analysis indicates that the proposed ultra-wideband band-stop filter can be designed for different lengths of resonators at similar transmission values. After obtaining the optimal geometric parameters for the basic filter design, the numbers of triangle resonators are increased to support the ultra-wideband band-stop filter feature of the design. For that purpose, three different designs are targeted in this study. Firstly, while increasing the number of triangle resonators, the dimensions of all resonators are equal.

Secondly, the structure is examined when the number and dimensions of the triangle resonators are increased.

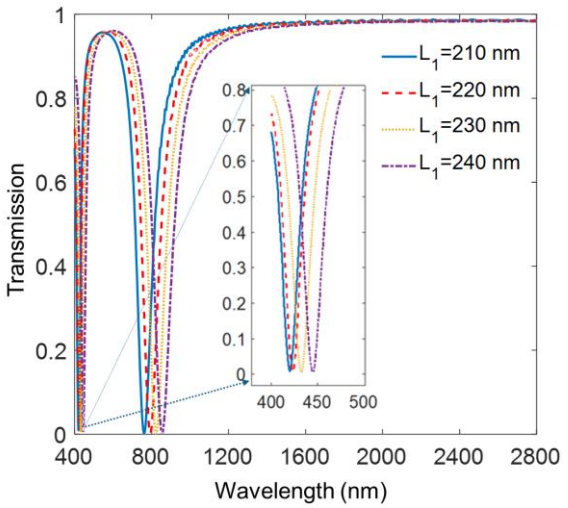

Figure 2. Parameter sweep analysis for the proposed structure.

Thirdly, while the number of triangle resonators is increased, the resonator size is kept constant and examined for the highest length value. Figure 3(a) visualizes the first band-stop filter design with six similar resonators. In this design, L_1 and L_2 lengths are 230 nm and 200 nm, respectively. w and d values are 50 nm. These four lengths are the same for all resonators. Figure 3(b) presents the transmission spectra for varied numbers (N) of the resonator. The wideband band-stop filter feature of the structure is improved by increasing the number of resonators from N=1 to N=6. When N=6, an ultra-wideband band-stop filter is obtained. These sweeps provide three different bandwidths which are $\Delta\lambda_1 = 37$ nm, $\Delta\lambda_2 = 119$ nm, $\Delta\lambda_3 = 619$ nm. This figure also shows the field distributions at 652 nm and 1100 nm where the transmission has high and low levels, respectively.

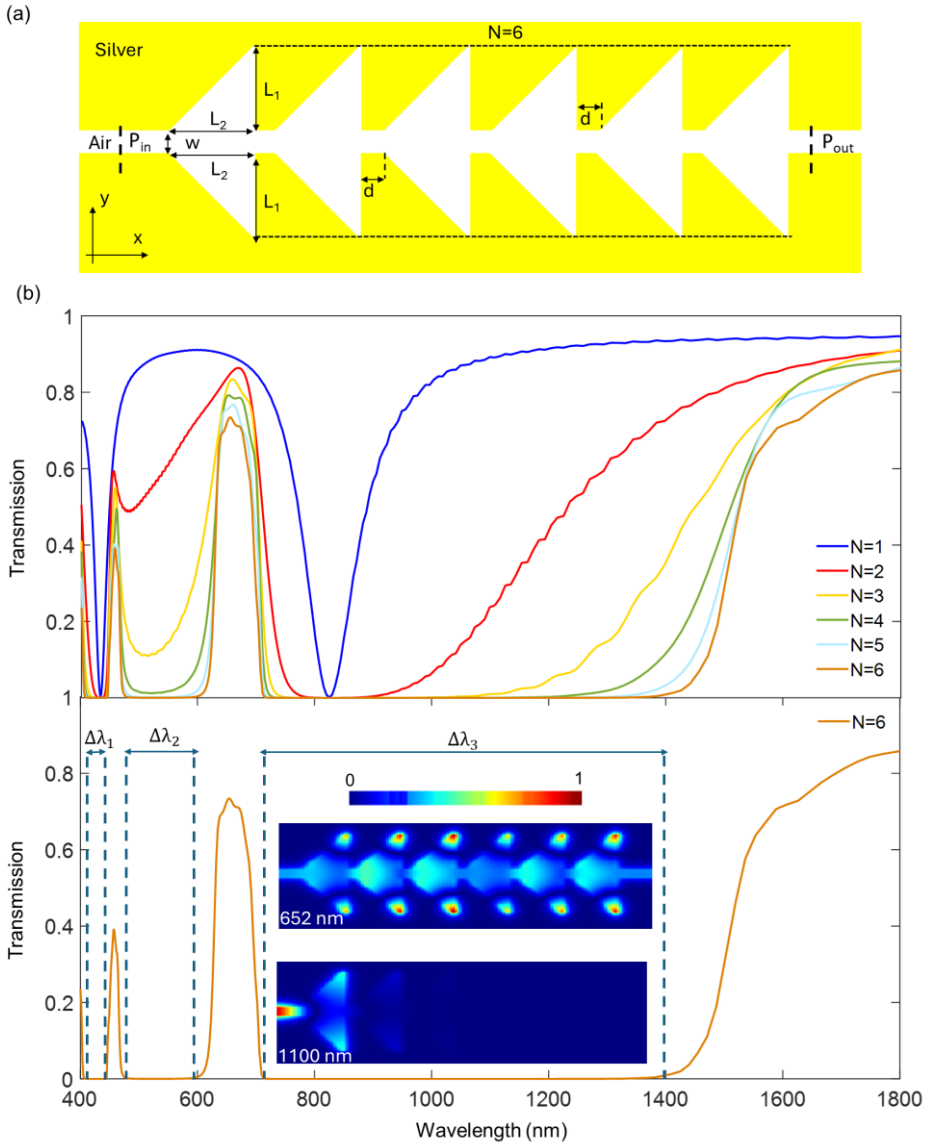

Figure 3. (a) The first proposed structure for the ultra-wideband band-stop filter. The x-axis length is 1.8 µm and the y-axis length is 1 µm for the structure. (b) The transmission spectra of the structure for the numbers of the resonator from N=1 to N=6. The transmission spectrum for N=6, three band-stop regions, and field distributions of the structure at 652 nm and 1100 nm, respectively.

When the design transmits the signal at 652 nm, the signal is not transmitted at 1100 nm. Figure 4(a) presents the second band-stop filter design that has six different resonators. In that design, L_x=200 nm and w=d=50 nm. y-axis lengths of the resonators are L_1=225 nm, L_2=250 nm, L_3=275 nm, L_4=300 nm, L_5=325 nm, and L_6=350 nm in this design. w and d values are 50 nm. Figure 4(b) visualizes the transmission spectra for varied numbers (N). The ultra-wideband band-stop filter behavior of the designed structure is developed by increasing the number of resonators from N=1 to N=6 and the y-axis lengths of the resonators. When N=6, the better ultra-wideband band-stop filter feature is achieved for this structure. These sweeps provide two different bandwidths which are $\Delta\lambda_1 = 308$ nm and $\Delta\lambda_2 = 837$ nm. When the second design is compared to the first design which has the same number of triangle resonators, the second one provides wider bandwidths for band-stop filtering.

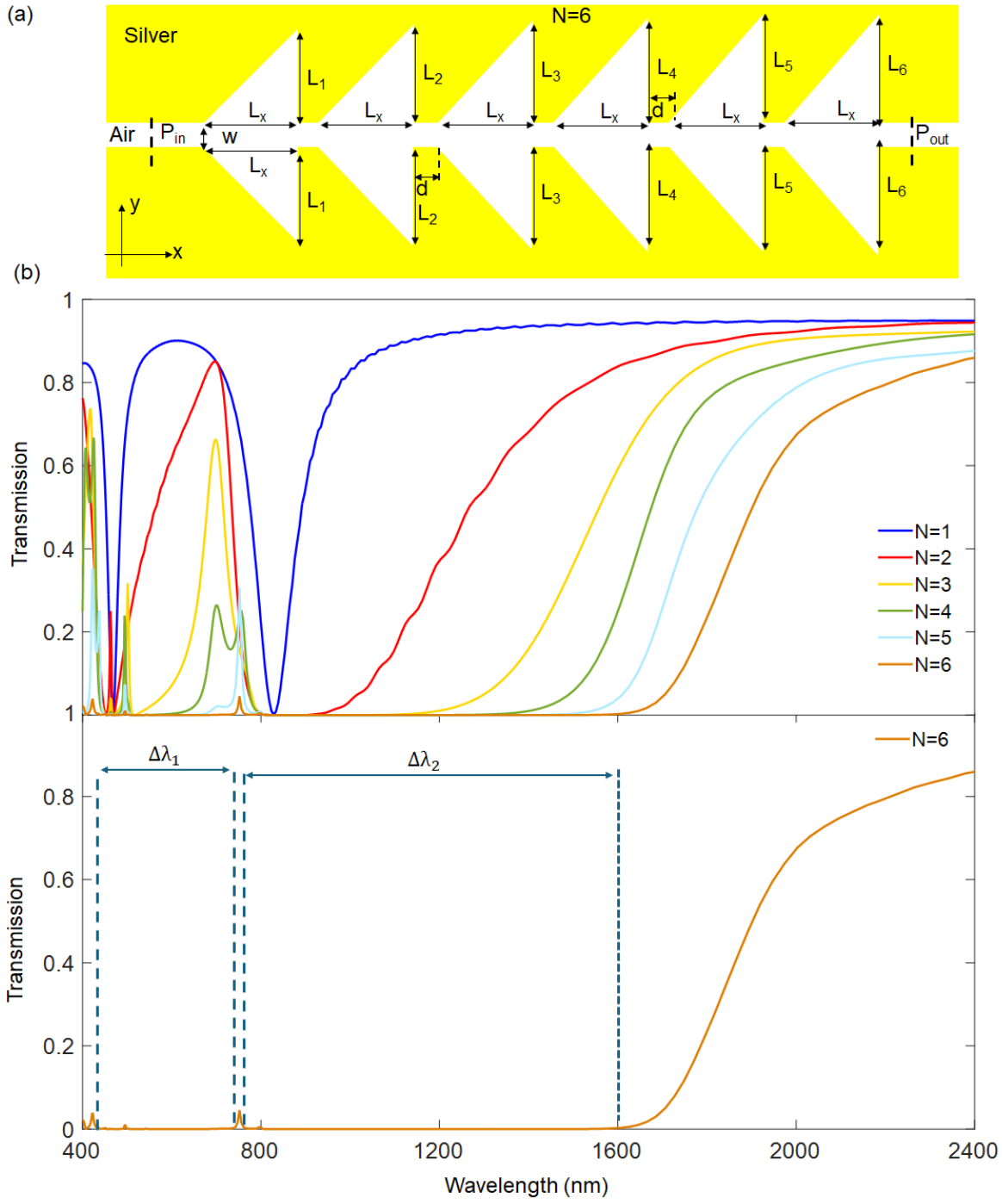

Figure 4. (a) The second proposed structure for the ultra-wideband band-stop filter. The x-axis length is 1.8 µm and the y-axis length is 1 µm for the structure. (b) The transmission spectra of the structure for the numbers of the resonator from N=1 to N=6. The transmission spectrum for N=6 and two band-stop regions.

Figure 5(a) illustrates the third band-stop filter design that has six similar resonators. L_6 and L_2 lengths are 350 nm and 200 nm, respectively. w and d values are 50 nm for this design. These four lengths are valid for all resonators. Figure 5(b) presents the transmission spectra of the proposed design for the numbers of the resonator from N=1 to N=6. Increasing the number of resonators from N=1 to N=6 in the design, the ultra-wideband band-stop filter feature of the proposed structure is further improved. When N=6, the best ultra-wideband band-stop filter is reached. These sweeps provide four different bandwidths $\Delta\lambda_1, \Delta\lambda_2, \Delta\lambda_3$ and $\Delta\lambda_4$ that are 24 nm, 65 nm, 218 nm, and 859 nm, respectively. When comparing the three designs with each other, the third structure shows higher bandwidths. As a result, increasing the lengths and the number of resonators provide better performance. Table 1 shows the results for the designed structures. In our study, when the maximum number of resonators is used, the design has a 1.8 µm × 1 µm size. A wider bandwidth can be achieved by increasing the size of the design and the number of resonators in it. In this case, the total structure size will increase. The most important parameter is to obtain the highest band-stop range using the maximum resonators at the minimum design size. Table 2 illustrates the performance comparison between the proposed study and previous studies in the literature.

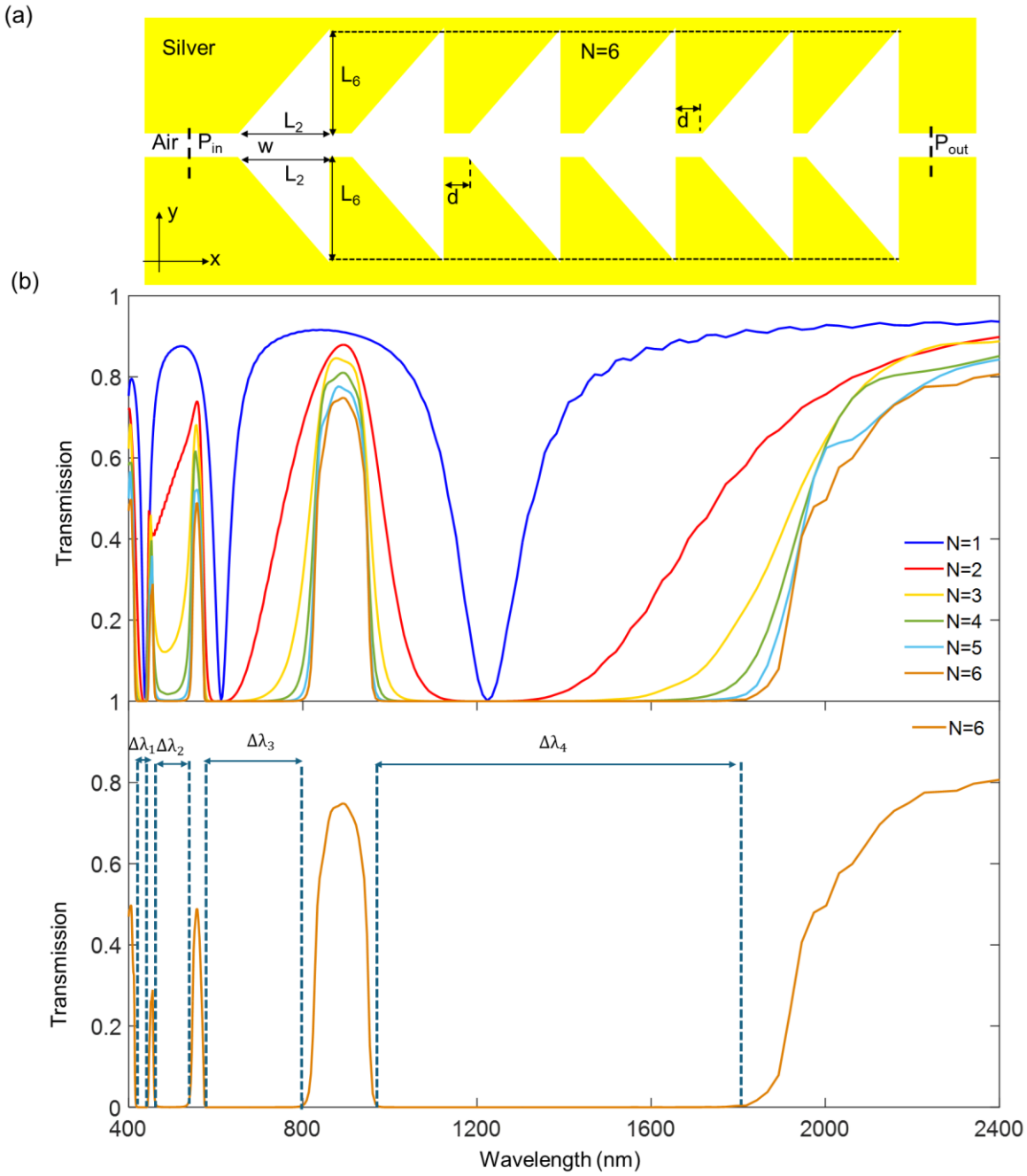

Figure 5. (a) The third proposed structure for the ultra-wideband band-stop filter. The x-axis length is 1.8 µm and the y-axis length is 1 µm for the structure. (b) The transmission spectra of the structure for the numbers of the resonator from N=1 to N=6. The transmission spectrum for N=6 and four band-stop regions.

Table 1. Comparison between the proposed structures in this study.

Design	Bandgap width	Total bandgap width	The resonator lengths
1	$\Delta\lambda_1$=37 nm, $\Delta\lambda_2$=119 nm, $\Delta\lambda_3$=619 nm	775 nm	Similar triangle resonators (L_1=230 nm)
2	$\Delta\lambda_1$=308 nm, $\Delta\lambda_2$= 837 nm	1145 nm	Different triangle resonators (L_1= 225 nm-350 nm)
3	$\Delta\lambda_1$=24 nm, $\Delta\lambda_2$=65 nm, $\Delta\lambda_3$=218 nm, $\Delta\lambda_4$=859 nm	1166 nm	Similar triangle resonators (L_1=350 nm)

Table 2. Comparison between the proposed study and previously reported studies.

Reference	Band-stop center wavelength (nm)	Maximum bandgap width (nm)	The resonator type
Lu *et al.* 2012	850	100	Side-coupled cavities and stub shaped
Chen *et al*. 2016	840	120	Single stub shaped
Li and Jiao 2019	1550	202	Tooth-shaped
Tao *et al*. 2010	1625	250	Double-sided teeth shaped
Yu *et al*. 2020	1020	340	Trapezoidal-shaped
Zegaar *et al*. 2022	2675	350	Triangular-shaped
Wang *et al*. 2016	1500	750	Multiple-teeth shaped
Zegaar *et al.* 2024	2825	1650	Hexagonal-shaped
This study	1395	859	Triangle-shaped

4. Conclusion

In this study, tunable ultra-wideband band-stop filters based on a metal-insulator-metal waveguide with triangle resonators have been proposed and analyzed. The results provide zero transmission values in visible and infrared regimes with ultra-wideband regions. The largest bandwidth is 308 nm in visible and 859 nm in infrared regimes for this study. Increasing the number of adjacent resonators to the waveguide improves the yields of the filters in terms of lower transmission values and wider bandwidths. The presented tunable ultra-wideband band-stop filters can be used effectively for light control applications with their high-performance parameters.

Declaration of Ethical Standards

The authors declare that they comply with all ethical standards.

Credit Authorship Contribution Statement

Author-1: Conceptualization, investigation, methodology and software, visualization and writing – original draft, supervision, and writing – review and editing

Declaration of Competing Interest

The authors have no conflicts of interest to declare regarding the content of this article.

Data Availability Statement

All data generated or analyzed during this study are included in this published article.

Acknowledgement

The author would like to thank the referees and the editor who contributed to the development of the article for their valuable opinions.

5. References

Al Mahmud, R., Faruque, M. O. and Sagor, R. H., 2021. A highly sensitive plasmonic refractive index sensor based on triangular resonator. *Optics Communications*, **483**, 126634. https://doi.org/10.1016/j.optcom.2020.126634

Chao, C. T. C., Chau, Y. F. C., Kooh, M. R. R., Lim, C. M., Thotagamuge, R. and Chiang, H. P., 2022. Ultrawide bandstop filter with high sensitivity using semi-circular-like resonators. *Materials Science in Semiconductor Processing*, **151**, 106985. https://doi.org/10.1016/j.mssp.2022.106985.

Chen, Z., Li, H., Li, B., He, Z., Xu, H., Zheng, M. and Zhao, M., 2016. Tunable ultra-wide band-stop filter based on single-stub plasmonic-waveguide system. *Applied Physics Express*, **9(10)**, 102002. https://doi.org/10.7567/APEX.9.102002

Chou Chau, Y. F., Chou Chao, C. T., Huang, H. J., Kooh, M. R. R., Kumara, N. T. R. N., Lim, C. M. and Chiang, H. P., 2020. Ultrawide bandgap and high sensitivity of a plasmonic metal-insulator-metal waveguide filter with cavity and baffles. *Nanomaterials*, **10(10)**, 2030. https://doi.org/10.3390/nano10102030

Ebadi, S. M., Örtegren, J., Bayati, M. S. and Ram, S. B. 2020. A multipurpose and highly-compact plasmonic

filter based on metal-insulator-metal waveguides. *IEEE Photonics Journal*, **12(3)**, 1-9. https://doi.org/10.1109/JPHOT.2020.2974959

Ebadi, S. M. and Khani, S., 2023. Design of a tetra-band MIM plasmonic absorber based on triangular arrays in an ultra-compact MIM waveguide. *Optical and Quantum Electronics*, **55(6)**, 482. https://doi.org/10.1007/s11082-023-04756-2.

Haque, M. A., Rahad, R., Faruque, M. O., Mobassir, M. S. and Sagor, R. H. 2024. Numerical analysis of a metal-insulator-metal waveguide-integrated magnetic field sensor operating at sub-wavelength scales. *Sensing and Bio-Sensing Research*, **43**, 100618. https://doi.org/10.1016/j.sbsr.2023.100618.

Johnson, P. B. and Christy, R. W., 1972. Optical constants of the noble metals. *Physical Review B*, **6(12)**, 4370. https://doi.org/10.1103/PhysRevB.6.4370.

Kamari, M., Hayati, M. and Khosravi, S., 2021. Tunable infrared wide band-stop plasmonic filter using T-shaped resonators. *Materials Science in Semiconductor Processing*, **133**, 105983. https://doi.org/10.1016/j.mssp.2021.105983.

Kamari, M., Hayati, M. and Khosravi, S. 2021. Design of dual-wideband bandstop MIM plasmonic filter using multi-circular ring resonators. *Optical Materials*, **122**, 111678. https://doi.org/10.1016/j.optmat.2021.111678.

Korkmaz, S. 2024. Multiple ultra-narrow band-stop filters based on MIM plasmonic waveguide with nanoring cavities. *Physica Scripta*, **99(3)**, 035503. https://doi.org/10.1088/1402-4896/ad203d.

Li, H. and Jiao, R. Z., 2019. Plasmonic band-stop filters based on tooth structure. *Optics Communications*, **439**, 201-205. https://doi.org/10.1016/j.optcom.2019.01.017.

Lin, J., Bo, F., Cheng, Y. and Xu, J., 2020. Advances in on-chip photonic devices based on lithium niobate on insulator. *Photonics Research*, **8(12)**, 1910-1936. https://doi.org/10.1364/PRJ.395305.

Liu, Y., Tian, H., Zhang, X., Song, J. and Wang, B. 2024. Dual control all-optical switch based on MIM door-type waveguide. *Optics Communications*, **552**, 130072. https://doi.org/10.1016/j.optcom.2023.130072.

Lu, H., Liu, X., Wang, G. and Mao, D., 2012. Tunable high-channel-count bandpass plasmonic filters based on an analogue of electromagnetically induced transparency. *Nanotechnology*, **23(44)**, 444003. https://doi.org/10.1088/0957-4484/23/44/444003.

Luo, W., Cao, L., Shi, Y., Wan, L., Zhang, H., Li, S., Wang Y., Sun S., Karim M. F., Cai H., Kwe L. C. and Liu, A. Q., 2023. Recent progress in quantum photonic chips for quantum communication and internet. *Light: Science & Applications*, **12(1)**, 175. https://doi.org/10.1038/s41377-023-01173-8.

Mariselvam, V., Preethi, A. A. P. and Akilarasu, G., 2022. Etched Triangle Resonator Dual Band Microstrip Band Pass Filter. *Wireless Personal Communications*, **125(2)**, 1537-1544. https://doi.org/10.1007/s11277-022-09620-2.

Mohammadi, G., Orouji, A. and Danaie, M. 2023. Highly compact tunable hourglass-shaped graphene band-stop filter at terahertz frequencies. *Results in Optics*, **13**, 100575. https://doi.org/10.1016/j.rio.2023.100575.

Patel, S. K., Surve, J., Prajapati, P. and Taya, S. A., 2022. Design of an ultra-wideband solar energy absorber with wide-angle and polarization independent characteristics. *Optical Materials*, **131**, 112683. https://doi.org/10.1016/j.optmat.2022.112683.

Tao, J., Huang, X. G., Lin, X., Chen, J., Zhang, Q. and Jin, X., 2010. Systematical research on characteristics of double-sided teeth-shaped nanoplasmonic waveguide filters. *Journal of the Optical Society of America B*, **27(2)**, 323-327. https://doi.org/10.1364/JOSAB.27.000323.

Tan, D., Wang, Z., Xu, B. and Qiu, J., 2021. Photonic circuits written by femtosecond laser in glass: improved fabrication and recent progress in photonic devices. *Advanced Photonics*, **3(2)**, 024002-024002. https://doi.org/10.1117/1.AP.3.2.024002.

Wang, H., Yang, J., Zhang, J., Huang, J., Wu, W., Chen, D. and Xiao, G., 2016. Tunable band-stop plasmonic waveguide filter with symmetrical multiple-teeth-shaped structure. *Optics letters*, **41(6)**, 1233-1236. https://doi.org/10.1364/OL.41.001233.

Yu, S., Wang, S., Zhao, T. and Yu, J., 2020. Tunable ultra-width bandgap U-shaped band-stop filters of chip scale based on periodic staggered double-side trapezoidal resonators in a metallic nanowaveguide. *Optics Communications*, 463, 125439. https://doi.org/10.1016/j.optcom.2020.125439.

Zegaar, I., Hocini, A. and Khedrouche, D. 2022. *Plasmonic stop-band filter based on an MIM waveguide coupled with cavity resonators*. In Journal of Physics: Conference Series. Sozopol, Bulgaria, 012025.

Zegaar, I., Hocini, A., Harhouz, A., Khedrouche, D. and Salah, H. B., 2024. An ultra-wideband bandstop plasmonic filter in mid-infrared band based on metal-insulator-metal waveguide coupled with an hexagonal resonator. *Journal of Optics*, **53**, 272–281. https://doi.org/10.1007/s12596-023-01138-5.

Zeng, L., Li, J., Cao, C., Li, X., Zeng, X., Yu, Q., Wen K., Yang J. and Qin, Y. 2022. An integrated-plasmonic chip of Bragg reflection and Mach-Zehnder interference based on metal-insulator-metal waveguide. *Photonic Sensors*, **12(3)**, 220303. https://doi.org/10.1007/s13320-022-0650-0.

Zhang, J., Feng, H., Ran, L., Gao, Y. 2022. Theoretical design and analysis of multichannel plasmonic switch based on triangle resonator combined with silver bar. *Optics Communications*, **520**, 128437. https://doi.org/10.1016/j.optcom.2022.128437.

Internet References

1- http://www.lumerical.com, (05.01.2024)